Random Number Generation with Cosmic Photons

Cheng Wu,[1,2] Bing Bai,[1,2] Yang Liu,[1,2] Xiaoming Zhang,[3] Meng Yang,[1,2] Yuan Cao,[1,2] Jianfeng Wang,[3] Shaohua Zhang,[4] Hongyan Zhou,[4] Xiheng Shi,[4] Xiongfeng Ma,[5] Ji-Gang Ren,[1,2] Jun Zhang,[1,2] Cheng-Zhi Peng,[1,2] Jingyun Fan,[1,2,*] Qiang Zhang,[1,2,†] and Jian-Wei Pan[1,2,‡]

[1]*Shanghai Branch, Department of Modern Physics and National Laboratory for Physical Sciences at the Microscale, University of Science and Technology of China, Shanghai 201315, China*

[2]*CAS Center for Excellence and Synergetic Innovation Center in Quantum Information and Quantum Physics, University of Science and Technology of China, Shanghai 201315, China*

[3]*Key Laboratory of Optical Astronomy, National Astronomical Observatories, Chinese Academy of Sciences, Beijing 100012, China*

[4]*Polar Research Institute of China, Shanghai 200136, China*

[5]*Center for Quantum Information, Institute for Interdisciplinary Information Sciences, Tsinghua University, Beijing 100084, China*

(Received 14 November 2016; published 5 April 2017)

Random numbers are indispensable for a variety of applications ranging from testing physics foundations to information encryption. In particular, nonlocality test provide strong evidence for our current understanding of nature—quantum mechanics. All the random number generators (RNGs) used for the existing tests are constructed locally, making the test results vulnerable to the freedom-of-choice loophole. We report an experimental realization of RNGs based on the arrival time of cosmic photons. The measurement outcomes (raw data) pass the standard NIST statistical test suite. We present a realistic design to employ these RNGs in a Bell test experiment, which addresses the freedom-of-choice loophole.

DOI: 10.1103/PhysRevLett.118.140402

Introduction.—Randomness is one of the most fundamental features of nature. The best example may be biological diversity [1]. Another example is Brownian motion [2,3], which has been studied for nearly two centuries. Random number generators (RNGs) are based on either a classical mechanism or a quantum process. Quantum random number generators (QRNGs) rely on breaking quantum superposition results into an unpredictable measurement outcome and are therefore deemed to be truly random. A number of quantum processes are utilized to make QRNGs (for reviews see Refs. [4,5] and references therein).

Bell tests, or experimental violation of Bell's inequality, provide strong support for quantum mechanics, especially to rule out local hidden variable models. Recently, both locality and efficiency loopholes were closed in Bell test experiments [6–8], in which QRNGs were employed in state measurements at two remote test sites. However, the test results may not be reliable if the two RNGs are somehow correlated (with each other and/or with the two physical devices). For instance, the distant entangled photon pairs in a Bell test learn the random inputs before they are separated. This is called a freedom-of-choice loophole (also known as a randomness loophole). The time constraint for a local hidden variable mechanism to occur to affect the test results in previous loophole free Bell experiments is less than 10^{-5} s before the experiment, which may be pushed deep into the cosmic history by adopting the RNG scheme based on cosmic photon measurements to take advantage of randomness at remote celestial objects, e.g., measuring the temporal mode of photons as studied in this Letter. The randomness of the outcomes cannot be proven strictly, but is supported by following physical observations. First, the setup measures the arrival time of photons from the celestial object which the telescope points at. Second, the generation time of cosmic photons from a celestial object is random, so is the arrival time. The states of photons from two celestial objects are independent. This is related to the no-signaling assumption. In a way, we assume that the nature is not malicious to jeopardize our experiment. We realize RNGs with photons from an array of cosmic radiation sources with magnitude between 4.85 and 13.5 and distance (from Earth) between 756 and 7.49×10^8 light years (ly). These RNGs can deliver raw random bits exceeding $10^6\ \mathrm{s}^{-1}$, which pass the NIST statistical test suite. We present a realistic design of event-ready Bell test experiments with these RNGs to address the freedom-of-choice loophole while closing locality and efficiency loopholes simultaneously.

Random number generation with cosmic photons.—The experiment is conducted in the Astronomy Observatory at Xinglong, China (N 40°23.75′, E 117°34.5′). We use a Ritchey-Chretien (RC) optical telescope with a diameter of 1 m and a focal length of $f = 5$ m to collect light from the cosmic radiation source under study (CRSS) and use prisms to direct light of various spectral bands to different applications (see Fig. 1). The light that is incident onto this RC telescope from a typical cosmic radiation source with

TABLE I. Photon counting data for cosmic radiation sources under study (see Supplemental Material for distance [10]) [23–25]

Name	Magnitude	Distance (ly)	Signal rate ($\times 10^6$ s^{-1})	total Data (Gb)	background (s^{-1})	r	min-entropy H
HIP15416 [23]	4.85	1177	2.20–2.28	1	914	2450	0.9969
HIP117447 [23]	5.43	6151	0.86–1.2	1	512	2012	0.9978
HIP2876 [25]	5.75	2675	0.51–0.53	1	464	1130	0.9981
HIP6522 [25]	6.07	5488	0.48–0.68	1	578	1010	0.9983
HIP3030 [23]	6.75	5344	0.64–0.65	1	518	1260	0.9976
HIP100548 [23]	7.03	5621	0.33–0.52	1	615	680	0.9973
HD33339 [25]	7.99	756	0.23–0.24	1	662	350	0.9980
HIP20276 [25]	8.24	1835	0.18–0.26	1	486	400	0.9980
HIP3752 [25]	9.02	908	0.12–0.13	1	532	235	0.9973
HIP114579 [25]	9.27	1967	0.05–0.10	1	442	170	0.9974
HIP117690 [25]	9.9	21733	0.033–0.043	1	674	57	0.9938
HIP23114 [25]	10.6	2243	0.009–0.013	0.1	417	28	0.9909
IGR J03334 + 371 [24]	13.5	7.49×10^8	0.0011–0.0031	0.1	359	8	0.9897

an angular spread of $\phi = 3''$ has a $1/e$ diameter of 73 μm and a numerical aperture (NA) of 0.10 at the focal plane. A multimode optical fiber with NA $= 0.22$ and a core diameter of 105 μm is placed at the focal plane to collect light with wavelength in the range, [680, 830] nm, and direct the light to a single photon avalanche diode (SPAD, model: EXCELITAS, active area: 170 μm, single photon detection efficiency: ~55% at 780 nm). A CCD camera is also placed at the focal plane to image the CRSS by detecting light with wavelength in the range, [530, 680] nm. We stabilize the coupling of cosmic photons from the CRSS into the multimode fiber by a standard altitude-azimuth tracking mechanism [9]. We estimate the total detection efficiency of a single cosmic photon to be about 2% (see Supplemental Material [10]). So we require an assumption that the detected photons represent a fair sample of photons emitted by the CRSS. In addition, as we assume in the above that the nature does not maliciously jeopardize our experiment, we assume that the propagation of cosmic photons and their arrival times are not affected by any mechanism other than the known mechanisms in astronomy studies such as refraction through slowly varying interstellar and intergalactic media and assume that the effect is identical for all photons [14]. In fact, there was no astronomy report on delaying the cosmic photon arrival time at the visible or near infrared wavelength [15]. We consider a major delay may be due to the refractive index of atmosphere around us and include it in the discussion below.

We choose to detect cosmic photons over a bandwidth of 150 nm to increase the rate of random bits, which features the Poissonian statistics: the mean photon number is a constant for equal time and the time interval between photon emission events is random. If the period T_W of a reference clock is equally divided into N time bins, the probability for a cosmic photon to arrive at an arbitrary time bin t_i $(i = 1, 2, \ldots, N)$ is a constant, $P_i = 1/N$. In our experiment, the photon-detection signal from the SPAD is recorded using a homemade time-to-digital converter (TDC) with a time resolution of 25 ps. We set $T_W =$ 40.96 ns to be smaller than the recovery time (45 ns) of the SPAD such that there is at most one detection event per clock cycle, and set $N = 256$ ($\times 160$ ps). We assign each time bin with a unique 8-bit binary code, and record the assigned code for the time bin in which a detection event occurs.

We study RNGs with photons from an array of celestial objects. The main results are summarized in Table I. First, we notice that the photon counting signal rates exceed 10^6 s^{-1} (which is within the linear operation mode of the SPAD in use) for CRSS with lower magnitude, demonstrating that this method is as efficient as laser-based RNGs in generating random numbers [16–22]. Second, despite the dramatic fluctuation of signal rates (shown by signal ranges

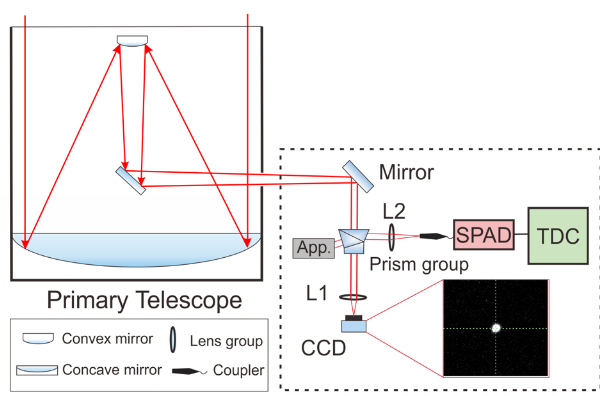

FIG. 1. Random number generation with cosmic photons. Photons from a cosmic radiation source under study with wavelength in the range [680, 830] nm are collected into a multimode optical fiber for RNG. Inset: Photons with wavelength in the range [530, 680] nm, form an image of the CRSS, here, quasar IGR J03334 + 371 is on the camera for tracking. Astronomy applications (APP).

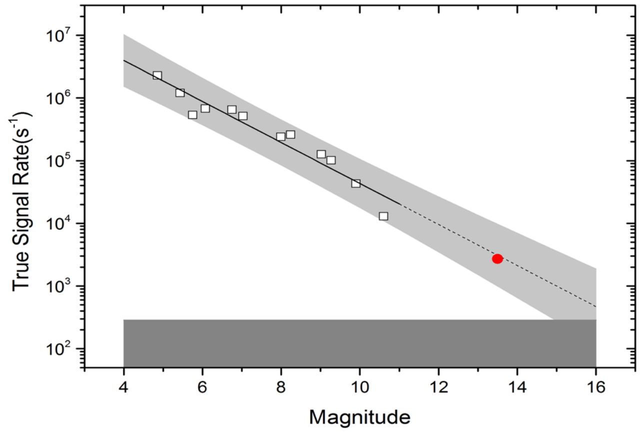

FIG. 2. Experimental true signal rate (background subtracted) versus magnitude. The trend line (solid) is fitted with data (open square) for magnitude <11, and extrapolated to magnitude 16 (dashed line). The shaded regions indicate 2 standard deviations, with the one on the horizontal axis for background. Solid red dot: data for quasar IGR J03334 + 371.

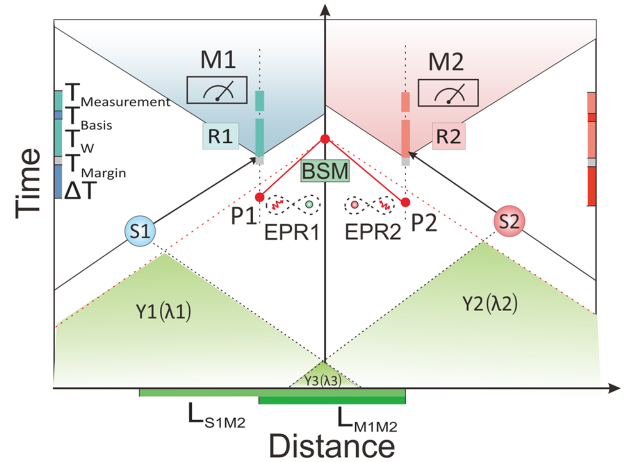

FIG. 3. Space-time diagram of an event-ready Bell test experiment with NV centers [6,14]. $S1$ and $S2$ are cosmic photon emission events, followed by events $R1$ and $R2$ to output random bits for base choice. $P1$ and $P2$ are events for NV centers to send photons for Bell state measurement after the creation of entangled photon-electron pairs (EPR1,2) at NV centers. The photons are sent for BSM via optical fibers, shown by red lines. A destructive BSM with photons from the two entangled electron-photon pairs prepares the two electrons in a Bell state, which is ready for state measurements ($M1$ and $M2$) after the base choice. $Y1$, $Y2$, and $Y3$ are local correlation events (denoted by local hidden variables, $\lambda 1$, $\lambda 2$, $\lambda 3$) that may occur in the overlapped region formed by the past light cones (see text for details).

in Table I), the true signal rate (with background subtracted) scales with magnitude as expected, as indicated in Fig. 2. We attribute fluctuation in the rate partly to atmospheric disturbance. Besides attenuating cosmic light, atmospheric disturbances deteriorate the coupling of light from CRSS into the multimode fiber by either displacing the focal position or modifying the beam profile, which cannot be corrected by the current tracking mechanism. We use the maximum rate for each CRSS to suppress such impact in generating the trend line. [We do not use the data for quasar IGR J03334 + 371 (solid red dots) in generating the trend line because of small signal-to-noise ratio.]

We use raw data in the analysis. For each CRSS, the probability of photon arrival time (P_i) is uniformly distributed around the ideal value of $1/256$, indicating a good level of randomness (see Supplemental Material [10]). We apply two standard methods to evaluate the performance of cosmic photon RNGs. The min-entropy $H_\infty = -\log(\max P_i)$ is consistent with the ideal value of 1 within 1%, and the raw data pass the NIST statistical test suite [26] (see Supplemental Material [10]). These two results certify the quality of these cosmic RNGs.

To estimate the background contribution, we point the RC telescope slightly away from the CRSS (at a dark patch of the sky) until the detection rate drops to a stable level. The background may include contributions due to detector dark counts or ground-based light sources, which can be used by local hidden variable theories and must be made insignificant. Below we present a realistic analysis on the Bell experiment with cosmic RNGs with large signal-to-noise ratio.

Event-ready Bell test experiment with cosmic RNGs.— The celebrated Bell's inequality [27,28] is based on the assumption of locality, realism, and freedom of choice. In previous Bell test experiments [6–8] with a pair of entangled particles A and B, the events for entanglement generation, base choices, and state measurements are separated space-like in future light cones. However, these light cones cross each other in $<10^{-5}$ s in the past direction, allowing the possibility for local correlation events occurring in the overlapped regions to control measurement outcomes. Furthermore, it was shown that a Bell test experiment is vulnerable to local hidden variable theories even with a conspiracy of as little as $1/22$ bit of mutual information between RNGs and source of entanglement [29]. Here, we consider two possible scenarios that local correlation events may impact the experimental outcomes as shown in Fig. 3. In the first case, a local correlation event $Y1(Y2)$ may share information, denoted by a local hidden variable $\lambda 1$ ($\lambda 2$), about photon emission event $S1(S2)$ for random bit generation with the source, prior to state preparation, provided that local correlations take place ahead at least by an amount of time $\tau_1 \geq \min(L_1/c, L_2/c)$, where L_1, L_2 are distances of the two cosmic sources from Earth. In the second case, a local correlation event (denoted by a hidden variable $\lambda 3$) may occur in the overlapped region formed by the past light cones of two cosmic photon radiation events, $S1$ and $S2$, prior to the experiment by $\tau_2 \geq (L_1 + L_2 + L_{12})/2c \geq \tau_1$, where L_{12} is the distance between the two cosmic sources (see Supplemental Material [10]). Therefore, local correlation events in the green shaded regions may impact the

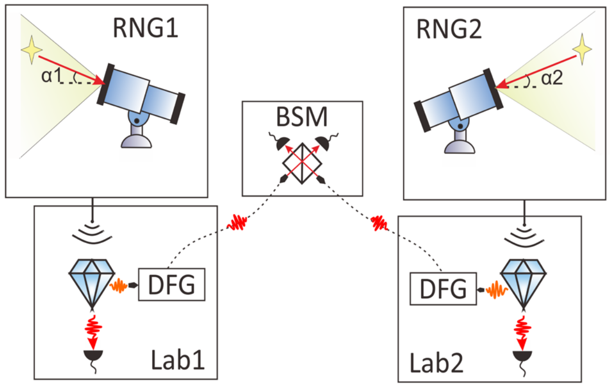

FIG. 4. Schematic of an event-ready Bell experiment. Each measurement station (Lab1 or Lab2) prepares an entangled electron-photon pair with a NV center. Lab1(2) down-converts single photons from visible to infrared (1550 nm) via difference frequency generation (DFG). A successful BSM with a single photon from Lab1 and a single photon from Lab2 projects the corresponding two electrons into a Bell state. RNG1 and RNG2 provide random bits per time window T_W to set the base in measuring the quantum state of the electron spin. $\alpha 1$ and $\alpha 2$ are angles of the optical axes of telescopes with respect to the Lab axis (see Supplemental Material [10]).

outcomes of the Bell test experiment as shown in Fig. 3, with the time constraint to be $\tau \geq \tau_1$. For example, by employing RNGs based on cosmic sources HIP 55 892 ($L_1 = 3325 \pm 1649$ ly, Magnitude 6.7) and and HIP 117928 ($L_2 = 3454 \pm 1433$ ly, Magnitude 8.9) [25], we have $\tau \geq 3325 \pm 1649$ yr (see Supplemental Material [10]), which is ~16 orders of magnitude improvement over previous loophole free Bell test experiments.

Below we present a realistic design to use the two RNGs (with signal-to-noise ratio >100) in an event-ready Bell test experiment with NV centers [6], as shown in Fig. 4.

First, locality requests spacelike separation between event of state measurement and event of base choice, which requires that the distance L_{M1M2} between two measurement stations Lab1 and Lab2 is set according to $T_W + T_{\mathrm{Basis}} + T_{\mathrm{Measurement}} + T_{\mathrm{Margin}} < L_{M1M2}/c \cos\alpha$, where T_{Basis} is the time elapsed for event completing the base choice upon receiving a random bit, $T_{\mathrm{Measurement}}$ is the time elapsed for event completing the state measurement after the base choice, T_{Margin} accounts for possible additional delays, and α is the elevation angle of the telescope (see Supplemental Material [10]). Taking $T_W = 8\ \mu$s, $T_{\mathrm{Measurement}} \sim 4\ \mu$s, $T_{\mathrm{Basis}} \sim 1\ \mu$s, $T_{\mathrm{Margin}} \sim 1\ \mu$s, and $\alpha \leq 30°$ for telescopes, we have $L_{M1M2} > 5$ km. Second, consideration of freedom of choice requests spacelike separation between event of cosmic photon emission and event of two-photon Bell state measurement (BSM), so photon-electron entanglement must be produced in the NV center in advance by $\Delta T > (1.45 - \cos\alpha) L_{M1M2}/2c \sim 5\ \mu$s, which is much shorter than the coherence time ($T\ 2 \sim 0.6$ s at 77 K [30]) of electron spin of the NV center (see Supplemental Material [10]).

Photons emitted by NV center at the visible wavelength (~640 nm) are down-converted to photons at the wavelength of ~1550 nm via DFG, because they are subject to high propagation loss in optical fiber. Considering a 1.5 dB loss due to the down-conversion operation [31] and a 1 dB loss due to photon propagation over the 5 km optical fiber, there is an improvement of ~10 dB in two-photon detection efficiency over the previous experiment [6]. With that, the averaged success probability per entanglement generation attempt is estimated to be $P_{\mathrm{total}} \sim 2.26 \times 10^{-8}$ (see Supplemental Material [10]). This will result in one event-ready electron pair entanglement per 0.29 h per 24 μs measurement period on average. So it will take about 72 h to violate the Bell's inequality with statistical confidence similar to the previous experiment [6]. More importantly, the time constraint for the local hidden variable mechanism to impact the outcome of the Bell test experiment is moved by more than 1000 years back into the past.

Discussions.—It was recently proposed to push the time constraint to reject local hidden variable mechanisms in a Bell test experiment by billions of years back into the cosmic history by employing RNGs with photons from quasars of high redshift [32]. We discuss about its practicability by analyzing the performance of a RNG with photons from quasar APM 08279 + 5255 with magnitude 15.3 and redshift $z = 3.91$. According to the trend line in Fig. 2, the true signal rate of this RNG is ~590 s^{-1} (at $\alpha = 30°$). We attribute the low signal-to-noise ratio ~2 (for background rate 550 s^{-1}) mainly to the optical system not being operated optimally. The signal-to-noise ratio can be increased to >50 by having the RC-telescope work in the diffraction limit [33], and >100 in the space due to reduced sky brightness and the absence of atmosphere attenuation to cosmic photons. The absence of atmospheric disturbance and angular separation of 180° between two telescopes are also advantages of a satellite-based cosmic Bell experiment (see Supplemental Material [10]).

Conclusion.—In conclusion, we realize cosmic-photon based RNGs and present a realistic design to use these RNGs in a Bell test experiment. We show that it is experimentally feasible to perform a Bell test experiment with RNGs based on quasars of high redshift, which will provide a strong support to quantum mechanics, by setting the time constraint to reject local hidden variable mechanisms deep into the cosmic history. Meanwhile, the method of single-photon detection of cosmic photons may provide a powerful tool for cosmology observation.

The authors would like to thank Z.-P. Li, D.-D. Li, X. Han, and X. Pan for technical assistance. We acknowledge the support of the staff of the Xinglong 1m telescope. This work has been supported by the National Fundamental Research Program Grant No. 2013CB336800, the Chinese Academy of Science, the National Natural Science

Foundation of China, and the Open Project Program of the Key Laboratory of Optical Astronomy, National Astronomical Observatories.

C. W. and B. B. contributed equally to this work.

Note added.—We became aware of a relevant work during the submission [34].

[*]fanjy@ustc.edu.cn
[†]qiangzh@ustc.edu.cn
[‡]pan@ustc.edu.cn

[1] L. H. Hartwell, J. J. Hopfield, S. Leibler, and A. W. Murray, Nature (London) **402**, C47 (1999).
[2] M. Kac, Am. Math. Mon. **54**, 369 (1947).
[3] H. Grabert and P. Talkner, Phys. Rev. Lett. **50**, 1335 (1983).
[4] X. Ma, X. Yuan, Z. Cao, B. Qi, and Z. Zhang, npj Quantum Inf. **2**, 16021 (2016).
[5] M. Herrero-Collantes and J. C. Garcia-Escartin, Rev. Mod. Phys. **89**, 015004 (2017).
[6] B. Hensen, H. Bernien, A. Dréau, A. Reiserer, N. Kalb, M. Blok, J. Ruitenberg, R. Vermeulen, R. Schouten, C. Abellán *et al.*, Nature (London) **526**, 682 (2015).
[7] L. K. Shalm, E. Meyer-Scott, B. G. Christensen, P. Bierhorst, M. A. Wayne, M. J. Stevens, T. Gerrits, S. Glancy, D. R. Hamel, M. S. Allman *et al.*, Phys. Rev. Lett. **115**, 250402 (2015).
[8] M. Giustina, M. A. Versteegh, S. Wengerowsky, J. Handsteiner, A. Hochrainer, K. Phelan, F. Steinlechner, J. Kofler, J.-Å. Larsson, C. Abellán *et al.*, Phys. Rev. Lett. **115**, 250401 (2015).
[9] S. H. Kwok, T. Krasuski, J. Lyke, J. Mader, K. McCann, and K. Tsubota, in *SPIE Astronomical Telescopes+ Instrumentation* (International Society for Optics and Photonics, Bellingham WA, 2016), p. 991305.
[10] See Supplemental Material at http://link.aps.org/supplemental/10.1103/PhysRevLett.118.140402 for space-time arrangement for the experiment and test results of random number, which includes Refs. [11–13].
[11] M. A. C. Perryman, L. Lindegren, J. Kovalevsky, E. Hoeg, U. Bastian, P. L. Bernacca, M. Crézé, F. Donati, M. Grenon, M. Grewing *et al.*, Astron. Astrophys. **323**, L49 (1997).
[12] A. Berk, L. S. Bernstein, and D. C. Robertson, MODTRAN: A moderate resolution model for LOWTRAN, Tech. Rep. (DTIC Document, 1987).
[13] J.-C. Zhang, L. Ge, X.-M. Lu, Z.-H. Cao, X. Chen, Y.-N. Mao, and X.-J. Jiang, Publ. Astron. Soc. Pac. **127**, 1292 (2015).
[14] J. Gallicchio, A. S. Friedman, and D. I. Kaiser, Phys. Rev. Lett. **112**, 110405 (2014).
[15] J. M. Cordes, *In SETI2020: A Roadmap for the Search for Extraterrestrial Intelligence* (Moyer Bell, New York, 2002).
[16] T. Jennewein, U. Achleitner, G. Weihs, H. Weinfurter, and A. Zeilinger, Rev. Sci. Instrum. **71**, 1675 (2000).
[17] C. Gabriel, C. Wittmann, D. Sych, R. Dong, W. Mauerer, U. L. Andersen, C. Marquardt, and G. Leuchs, Nat. Photonics **4**, 711 (2010).
[18] T. Symul, S. Assad, and P. K. Lam, Appl. Phys. Lett. **98**, 231103 (2011).
[19] Y.-Q. Nie, H.-F. Zhang, Z. Zhang, J. Wang, X. Ma, J. Zhang, and J.-W. Pan, Appl. Phys. Lett. **104**, 051110 (2014).
[20] C. Abellán, W. Amaya, M. Jofre, M. Curty, A. Acín, J. Capmany, V. Pruneri, and M. Mitchell, Opt. Express **22**, 1645 (2014).
[21] M. Applegate, O. Thomas, J. Dynes, Z. Yuan, D. Ritchie, and A. Shields, Appl. Phys. Lett. **107**, 071106 (2015).
[22] C. Abellán, W. Amaya, D. Mitrani, V. Pruneri, and M. W. Mitchell, Phys. Rev. Lett. **115**, 250403 (2015).
[23] F. Van Leeuwen, Astron. Astrophys. **474**, 653 (2007).
[24] N. Masetti, E. Mason, L. Morelli, S. Cellone, V. McBride, E. Palazzi, L. Bassani, A. Bazzano, A. Bird, P. Charles *et al.*, Astron. Astrophys. **482**, 113 (2008).
[25] T. L. Astraatmadja and C. A. Bailer-Jones, Astrophys. J. **833**, 119 (2016).
[26] A. Rukhin, J. Soto, J. Nechvatal, M. Smid, E. Barker, S. Leigh, M. Levenson, M. Vangel, D. Banks, A. Heckert, J. Dray, and S. Vo, NIST Special Publication 800-22, Revision 1a (2010).
[27] J. S. Bell, Physics **1**, 195 (1964).
[28] J. S. Bell, *Speakable and Unspeakable in Quantum Mechanics: Collected Papers on Quantum Philosophy* (Cambridge University Press, New York, 1987).
[29] M. J. W. Hall, Phys. Rev. A **84**, 022102 (2011).
[30] N. Bar-Gill, L. M. Pham, A. Jarmola, D. Budker, and R. L. Walsworth, Nat. Commun. **4**, 1743 (2013).
[31] K. De Greve, L. Yu, P. L. McMahon, J. S. Pelc, C. M. Natarajan, N. Y. Kim, E. Abe, S. Maier, C. Schneider, M. Kamp *et al.*, Nature (London) **491**, 421 (2012).
[32] F. Saturni, D. Trevese, F. Vagnetti, M. Perna, and M. Dadina, Astron. Astrophys. **587**, A43 (2016).
[33] P. Wizinowich, D. Acton, C. Shelton, P. Stomski, J. Gathright, K. Ho, W. Lupton, K. Tsubota, O. Lai, C. Max *et al.*, Publ. Astron. Soc. Pac. **112**, 315 (2000).
[34] J. Handsteiner, A. S. Friedman, D. Rauch, J. Gallicchio, B. Liu, H. Hosp, J. Kofler, D. Bricher, M. Fink, C. Leung, A. Mark, H. T. Nguyen, I. Sanders, F. Steinlechner, R. Ursin, S. Wengerowsky, A. H. Guth, D. I. Kaiser, T. Scheidl, and A. Zeilinger, Phys. Rev. Lett. **118**, 060401 (2017).